Burns & Trauma, 2022, 10, tkac043
https://doi.org/10.1093/burnst/tkac043
Research Article

OXFORD

Research Article

HSP70 alleviates sepsis-induced cardiomyopathy by attenuating mitochondrial dysfunction-initiated NLRP3 inflammasome-mediated pyroptosis in cardiomyocytes

Chenlu Song[1,†], Yiqiu Zhang[1,†], Qing Pei[1], Li Zheng[2], Meiyu Wang[2], Youzhen Shi[3], Shan Wu[1], Wei Ni[4], Xiujun Fu[1], Yinbo Peng[1], Wen Zhang[1] and Min Yao[1,5,*]

[1]Department of Plastic and Reconstructive Surgery, Shanghai Ninth People's Hospital, Shanghai Jiao Tong University School of Medicine, 639 Zhizaoju Road, Shanghai, 200011, China, [2]Department of Ultrasound, Baoshan Integrated Traditional Chinese and Western Medicine Hospital, 28 Tuanjie Road, Shanghai, 201999, China, [3]Department of Ultrasound, Shanghai Ninth People's Hospital, Shanghai Jiao Tong University School of Medicine, 280 Mohe Road, Shanghai, 201999, China, [4]Wuhan National Laboratory for Optoelectronics, Huazhong University of Science and Technology, 1037 Luoyu road, Wuhan, 430000, China and [5]Institute of Traumatic Medicine, Shanghai Jiao Tong University School of Medicine Shanghai, 201999, China

*Correspondence. Email: my058@vip.sina.com

[†]These authors contributed equally to this work.

Received 6 December 2021; Revised 2 April 2022; Editorial decision 5 September 2022

Abstract

Background: Sepsis-induced cardiomyopathy (SIC) is an identified serious complication of sepsis that is associated with adverse outcomes and high mortality. Heat shock proteins (HSPs) have been implicated in suppressing septic inflammation. The aim of this study was to investigate whether HSP70 can attenuate cellular mitochondrial dysfunction, exuberated inflammation and inflammasome-mediated pyroptosis for SIC intervention.

Methods: Mice with cecal ligation plus perforation (CLP) and lipopolysaccharide (LPS)-treated H9C2 cardiomyocytes were used as models of SIC. The mouse survival rate, gross profile, cardiac function, pathological changes and mitochondrial function were observed by photography, echocardiography, hematoxylin–eosin staining and transmission electron microscopy. In addition, cell proliferation and the levels of cardiac troponin I (cTnI), interleukin-1β (IL-1β) and tumor necrosis factor-α (TNF-α) were determined by Cell Counting Kit-8, crystal violet staining and enzyme-linked immunosorbent assay. Moreover, mitochondrial membrane potential was assessed by immunofluorescence staining, and dynamin-related protein 1 and pyroptosis-related molecules [nucleotide-binding domain, leucine-rich-repeat containing family pyrin domain-containing 3 (NLRP3), caspase-1, gasdermin-D (GSDMD), gasdermin-D N-terminal (GSDMD-N)] were measured by western blotting, immunoprecipitation and immunoblotting. Finally, *hsp70.1* knockout mice with CLP were used to verify the effects of HSP70 on SIC and the underlying mechanism.

Results: Models of SIC were successfully established, as reduced consciousness and activity with liparotrichia in CLP mice were observed, and the survival rate and cardiac ejection fraction (EF) were decreased; conversely, the levels of cTnI, TNF-α and IL-1β and myocardial tissue damage were increased in CLP mice. In addition, LPS stimulation resulted in a reduction in cell viability, mitochondrial destabilization and activation of NLRP3-mediated pyroptosis molecules *in vitro*. HSP70 treatment improved myocardial tissue damage, survival rate and cardiac dysfunction caused by CLP. Additionally, HSP70 intervention reversed LPS-induced mitochondrial destabilization, inhibited activation of the NLRP3 inflammasome, caspase-1, GSDMD and GSDMD-N, and decreased pyroptosis. Finally, knockout *of hsp70.1* mice with CLP aggravated cardiac dysfunction and upregulated NLRP3 inflammasome activity, and exogenous HSP70 significantly rescued these changes. It was further confirmed that HSP70 plays a protective role in SIC by attenuating mitochondrial dysfunction and inactivating pyroptotic molecules.
Conclusions: Our study demonstrated that mitochondrial destabilization and NLRP3 inflammasome activation-mediated pyroptosis are attributed to SIC. Interestingly, HSP70 ameliorates sepsis-induced myocardial dysfunction by improving mitochondrial dysfunction and inhibiting the activation of NLRP3 inflammasome-mediated pyroptosis, and such a result may provide approaches for novel therapies for SIC.

Key words: HSP70, Sepsis-induced cardiomyopathy, Mitochondria destabilization, Inflammation, NLRP3 inflammasome, Pyroptosis

Highlights

- Exogenous HSP70 inhibits pyroptosis by attenuating mitochondrial destabilization, reducing proinflammatory cytokines and inactivating the NLRP3 inflammasome-mediated caspase-1 and GSDMD pathways in sepsis-induced cardiomyopathy.
- Application of HSP70 alleviates myocardial damage and protects against sepsis-induced cardiomyopathy *in vivo* and *in vitro*.
- Gene deficiency of HSP70 aggravates cardiac injury and mitochondrial dysfunction, upregulates activation of the NLRP3 inflammasome and pyroptosis, and leads to increased mortality of sepsis-induced cardiomyopathy.

Background

Sepsis refers to a systemic inflammation syndrome caused by various endogenous and exogenous pathogenic factors, leading to multiple organ dysfunction. Sepsis-induced cardiomyopathy (SIC) is one of the main complications of sepsis, with high mortality. The overall incidence rate of septic cardiomyopathy is as high as 40–60% in intensive care units, which seriously threatens the lives of patients worldwide. In the past few decades, despite improvements in antibiotic therapies and critical care techniques, current management for septic cardiomyopathy remains supportive care, and most molecule-based interventions have failed clinically [1–4]. Therefore, the exploration of new therapeutic approaches is urgently needed to develop novel treatments for this devastating situation. The mechanisms underlying SIC are not well known. Emerging evidence has demonstrated that inflammatory responses play crucial roles in the pathogenesis of septic cardiac injury. In addition, it is known that mitochondria comprise ~30% of myocardial volume, and inflammation triggers mitochondrial dysfunction of cardiomyocytes, which leads to an abnormal overproduction of mitochondrial-initiated danger-associated molecular patterns (DAMPs) [5]. These molecules exacerbate myocardial inflammation and initiate multiple cell death pathways, including pyroptosis, and myocardial dysfunction occurs sequentially during sepsis [6]. However, there is no clear understanding of the role and mechanism of mitochondrial-initiated pyroptosis in the pathogenesis of septic myocardial damage.

Accumulating evidence indicates that inflammasomes are involved in the damage of myocardial tissue [7–9]. The nucleotide-binding domain, leucine-rich-repeat containing family pyrin domain-containing 3 (NLRP3) inflammasome is a multiprotein intracellular complex that is activated upon infection and leads to caspase-1-dependent secretion of the proinflammatory cytokines tumor necrosis factor-α (TNF-α) and interleukin-1β (IL-1β) and a type of programmed proinflammatory cell death termed pyroptosis [10,11]. It is now clear that mitochondria play a pivotal role in NLRP3 initiation and activation via mitochondrial destabilization, membrane permeability, mitochondrion-derived molecules and the relevant signaling pathway [12]. Upon stimulation, NLRP3 is activated through the canonical or noncanonical pathway of the inflammasome, which in turn interacts with procaspase-1. Procaspase-1 clustering leads to autocleavage and the formation of active caspase-1, resulting in the induction of TNF-α and IL-1β and the occurrence of gasdermin-D (GSDMD)-mediated pyroptosis [13,14]. In particular, NLRP3 inflammasome activation is pathogenic and is associated with myocardial inflammation and sequential cardiomyopathy during sepsis [15].

The heat shock protein family (HSP) is a class of highly conserved proteins in eukaryotic and prokaryotic cells that participates in the cellular response to pathophysiological stress conditions. HSP70 is known as a major HSP and includes inducible and structural forms [16,17]. Inducible HSP70 exists in mitochondria and the plasmic reticulum and has emerged as a link between the immune response and various stresses [18]. Furthermore, current studies have reported that HSP70, as the most classic molecular chaperone, plays a crucial role in protecting cells from inflammation and injury by stabilizing the mitochondrial membrane [19,20]. Additionally, HSP70 controls the initiation of the NLRP3 inflammasome and the activation of caspases and pyroptotic molecules in pathogen-associated molecular patterns [21]. Some studies suggest that sepsis is a multifaceted immune response to pathogens involved in the activation of proinflammatory responses. Along this line, sepsis triggers pyroptosis, which can occur in multiple organs, including the heart [22]. Thus, HSP70 has been speculated to impede inflammatory pyroptosis and repair cardiac dysfunction and the underlying mechanisms require further elucidation. Evidence suggests that HSP70 can protect cardiomyocytes from sepsis-associated cardiomyopathy, myocardial ischemia–reperfusion injury, atherosclerosis, myocardial infarction and ischemic stroke [23–26]. Moreover, several clinical studies of HSP70 in patients showed that an increased level of HSP70 is a risk factor in patients with stroke [27]. Thus, HSP70 might be a target for diagnostics and therapy in different types of cardiovascular diseases [28]. Given the plethora of effects of HSP70, including stabilization of the mitochondrial membrane and function, inactivation of the NLRP3 inflammasome, and protection against pyroptosis, determining the precise role and mechanism of HSP70 in mitochondria and inflammatory pyroptosis during SIC is of crucial importance.

In this study, we established mouse and cell sepsis models with or without HSP70 to investigate animal survival, changes in myocardial function, mitochondrial stabilization of cardiomyocytes, the levels of proinflammatory cytokines and activation of NLRP3 inflammasome-mediated pyroptosis signaling *in vivo* and *in vitro*. We show that HSP70 ameliorates SIC by regulating the mitochondria-initiated NLRP3 inflammasome and repressing caspase-1–GSDMD–pyroptosis. Finally, gene deficiency in HSP70 mice with sepsis was utilized to verify the effect of HSP70. Our findings may provide potential therapeutic approaches for treating SIC.

Methods

Cell line and reagents

Recombinant human HSP70 (HSP70) protein was purchased from R&D Systems (AP-100-100, Minneapolis, MN, USA). Lipopolysaccharide (LPS) was purchased from Sigma–Aldrich (L2630, USA). The H9C2 cardiomyoblast cell line was purchased from the American Type Culture Collection (Rockville, MD, USA).

Cell culture

H9C2 cells were cultured in Dulbecco's modified Eagle's medium (DMEM; Gibco, CA, USA) supplemented with 10% fetal bovine serum (FBS; Gibco, CA, USA) and 1% penicillin–streptomycin (Gibco, CA, USA) in a humidified atmosphere at 37°C with 5% CO_2. To establish a sepsis model *in vitro*, H9C2 cells were treated with LPS (1 μg/ml for 24 h) and LPS + ATP (LPS, 1 μg/ml for 24 h; ATP, 5 mM for 2 h). To evaluate the protective effect of HSP70, H9C2 cells were pretreated with HSP70 (2.5 μg/ml) for 10 min before LPS stimulation (1 μg/ml).

Animals

The present animal study was approved by the Animal Ethics Committee of the Shanghai Ninth People's Hospital. C57BL/6 mice were purchased from Shanghai Laboratory Animal Center (China) and maintained in a standard, specific pathogen-free facility environment (22–24°C, 12 h light/dark cycle) with access to food and water. HSP70 (*hsp*70.1) knockout mice (C57BL/6) were generated by Cyagen Biosciences Inc. (Shanghai, China) through CRISPR/Cas9-mediated genome editing (serial number: KOCMP-15511-hsp70.1). Sepsis was induced by cecal ligation plus perforation (CLP) in mice as described in previous studies [29]. The experimental mice (6–8 weeks old, 20–25 g) were anesthetized by intraperitoneal injection of 1% sodium pentobarbital (100 mg/kg). Midline laparotomy was performed (~1 cm). The cecum was ligated below the ileocaecal valve with 4–0 silk ligatures and punctured using a 22-gauge needle. Then, the cecum was extruded with a small amount of feces and returned to the abdomen. The incision was closed. The sham mice underwent the same surgical procedures without ligation and puncture. After the operation, all mice received fluid resuscitation with 0.9% saline (mg/kg) by subcutaneous injection.

The C57BL/6 WT mice were assigned to four groups ($n = 6$): NC (normal control), sham, CLP and CLP + HSP70. In the CLP + HSP70 group, mice were injected in the inner canthus veniplex with 50 μg/kg recombinant human HSP70 protein 10 min before CLP. Mice were regularly observed for survival analysis in the following 3 days and quickly anesthetized to collect blood and cardiac tissue at 24 h after the operation for further evaluation. In another experiment, HSP70 knockout mice were divided into three groups ($n = 6$) with CLP: $hsp70.1^{+/+}$, $hsp70.1^{-/-}$ and $hsp70.1^{-/-}$ + HSP70.

Echocardiography

Transthoracic 4D M-mode echocardiogram and pulsed wave Doppler spectral tracings (EPIQ 5, PHILIP, The Netherlands) were used to measure left ventricular (LV) wall thickness, LV end-systolic diameter and LV end-diastolic diameter. The percentage ejection fraction (EF %) was calculated as described previously [30].

Enzyme-linked immunosorbent assay

Blood samples were collected at 24 h after CLP and then centrifuged at 3000 rpm for 15 min at room temperature to separate the serum. Myocardial enzyme cardiac troponin I (cTnI; R&D Systems, Inc. Minneapolis, MN, USA) and inflammatory factors (IL-1β, MultiSciences Biotech, Shanghai, China; TNF-α, BioAssay Systems, Hayward, CA) were determined using commercial enzyme-linked immunosorbent assay (ELISA) kits. In addition, inflammatory factors (IL-1β, TNF-α) in the culture media of H9C2 cells were measured by ELISA according to the manufacturer's instructions.

Histology and immunohistochemistry (hematoxylin–eosin and connexin 43 staining)

Mice were sacrificed to collect myocardial tissues, which were immersed in paraformaldehyde and prepared for paraffin-based slices (5 μm). After dewaxing, hydrogen peroxide treatment and staining with hematoxylin–eosin (H&E) and connexin 43 (CX43) (1: 100; 3512S; CST) antibody, polymer enhancer and enzyme-labeled anti-rabbit/rat polymers were added. Subsequently, counterstaining, dehydration and mounting were performed. An optical microscope (Nikon TE2000-U; Japan) was used for histological evaluations. Three sections per heart were examined, depending on the absence of myofibrillar loss. ImageJ was used to quantify cardiomyocyte size (mm^2) at 20× magnification via captured pictures.

Transmission electron microscopy

Dissected cardiac tissue was fixed in 2.5% glutaraldehyde in a 0.1 M phosphate buffer (pH = 7.4) for 24 h at room temperature. After fixation, the material was rinsed several times with a mixture of 50 ml of 0.1 M phosphate buffer (pH = 7.4) and 50 ml of ddH_2O to which 4.6 g of saccharose was added. The material was postfixed for 2 h in a mixture of 1% OsO4 in a 0.1 M phosphate buffer (pH = 7.4) and dehydrated in a graded series of ethanol, which was replaced by acetone. After using uranyl acetate for 15 min and lead citrate for 20 min, ultrathin sections (70 nm thick) were examined using a Hitachi H500 transmission electron microscope. Three sections per heart were examined and damaged mitochondria were quantified in captured pictures.

Propidium iodide staining

Cells were incubated with propidium iodide (PI) (BL116A, Biosharp) at a concentration of 0.1 mg/ml in 0.01 M phosphate buffered saline (PBS), pH 7.2, for 30 min at room temperature in the dark. The slides were thoroughly washed in PBS and observed under a confocal microscope (TCS SP8, Leica, Germany).

Cell proliferation assay

Cell viability was measured by a Cell Counting Kit-8 (CCK8, Beyotime, Shanghai, China). In brief, cells were seeded in 96-well plates. CCK8 solution (10 μl) was added to each well and incubated for 2 h at 37°C. Subsequently, the optical density (OD) value in each well was determined at an absorbance of 450 nm using a microplate reader (Tecan, Switzerland) to analyze different cell groups. Crystal violet staining was used to screen cell survival and death. H9C2 cells were seeded in a 6-well plate and incubated for 2–3 days at 37°C. After aspirating the medium and washing the cells twice with phosphate buffered saline (PBS), the cells were dyed with 1 ml of 0.5% crystal violet staining solution in each well for 20 min at room temperature. Then, the plate was washed and air-dried for 16–24 h at room temperature. After incubating with 1 ml of methanol for 20 min and washing, images of the plate were taken by a digital camera (Nikon J2). The density was calculated by ImageJ software (National Institutes of Health, MD, USA). All experiments were performed in triplicate.

Confocal microscopy of mitochondria stained by immunofluorescence (JC-1 and MitoTracker Green)

H9C2 cell monolayers were maintained in a well of a six-well culture plate and washed twice with PBS. After the medium was aspirated, 500 nM MitoTracker Green (C1048, Beyotime, China) or 5 μM JC-1 (C2006, Beyotime, China) was added to the well. Then, the cells were incubated for 45 min at 25°C in the dark on a vibrator with a vibrating velocity of ~30 turns per min. After staining, the cells were washed with PBS three times for 20 min each time and then observed with a confocal microscope (TCS SP8, Leica, Germany).

Western blotting

Both cardiac tissue and H9C2 cells were lysed in RIPA lysis buffer containing protease inhibitor cocktail. Protein concentrations were measured using a bicinchoninic acid (BCA) protein assay kit (Invitrogen, USA). The same amounts of protein samples were separated by 10% sodium dodecyl sulfate-polyacrylamide difluoride (SDS–PAGE) membranes and transferred to polyvinylidene fluoride membranes (PVDF) (Millipore, MA, USA). After blocking with 5% nonfat milk at RT for 1 h, membranes were incubated with primary antibodies against HSP70 (1:1000; ab79852, Abcam), Gasdermin-D (GSDMD,1:1000; ab219800, Abcam), Gasdermin-D N-terminal (GSDMD-N; 1:1000; ab215203, Abcam), Glyceraldehyde-3-phosphate dehydrogenase (GAPDH, (1:1000; ab9485, Abcam), caspase 1 (1:1000; abs131519, Absin), NOD-like receptor thermal protein domain associated protein 3 (NLRP3, (1:1000; ab151715, Absin), Connexin 43 (CX43, (1:8000, C6219, Sigma) and Dynamin-related protein 1 (DRP1, (1:1000; Ab-DF7037, Affinity) overnight at 4°C. After washing with Tris-buffered saline Tween-20 (TBST) buffer the next day, the membranes were incubated with secondary antibodies (goat anti-rabbit IgG, 1:5000, ab205718, Abcam) at RT for 2 h. Finally, the protein bands were detected using a chemiluminescence detection kit (Thermo Fisher Scientific, USA) and a Fusion-capture system (Fusion, France).

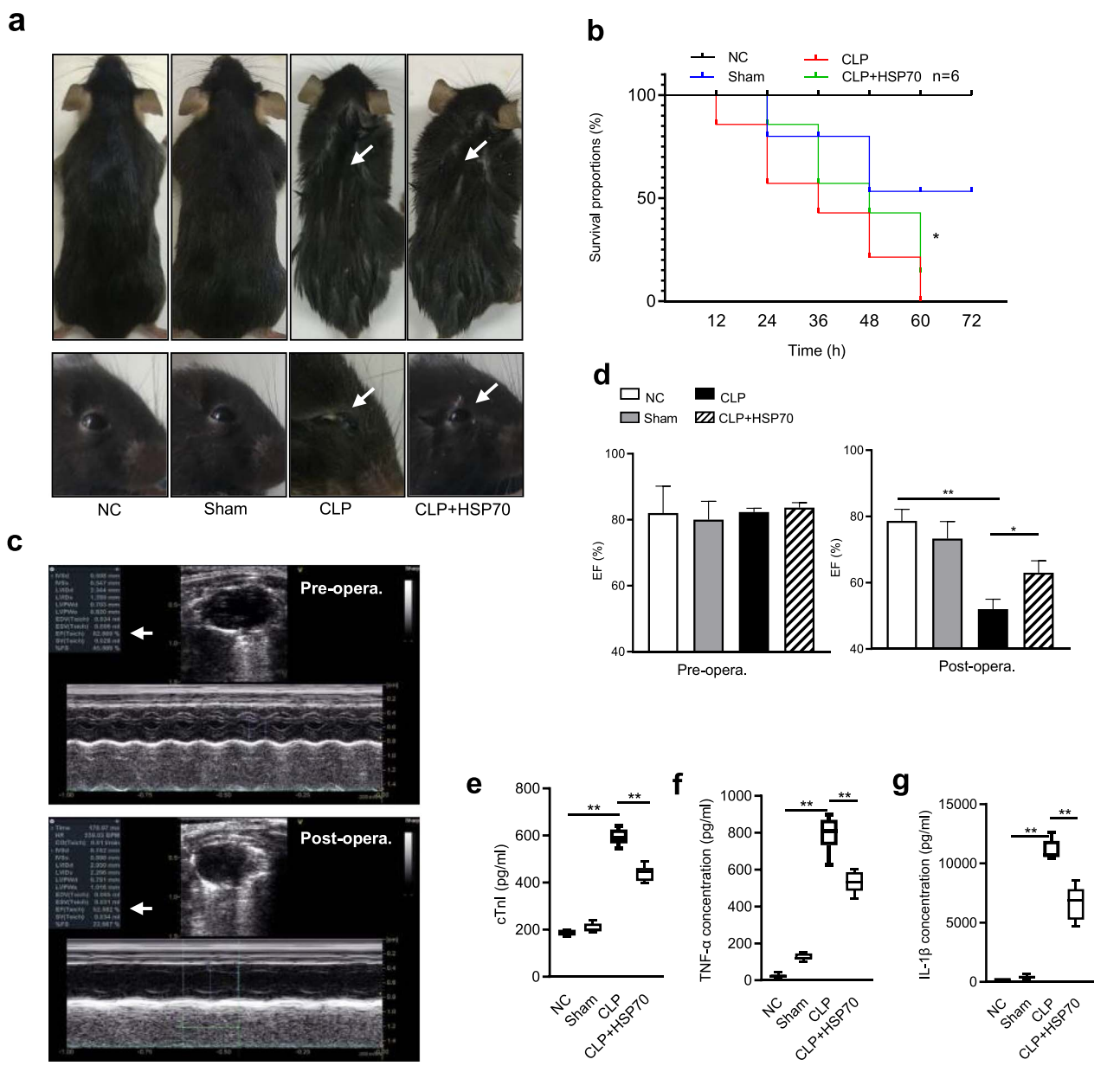

Figure 1. HSP70 improves cardiac function and attenuates inflammation in sepsis-induced cardiomyopathy *in vivo*. (**a, b**) C57BL/6 WT mice were assigned to four groups: NC, sham, CLP and CLP + HSP70. Gross profile, periocular secretions and liparotrichia as indicated with white arrows and survival rate were observed (CLP *vs* CLP + HSP70, $^{*}p < 0.05$). (**c, d**) ECG was performed to measure EF and representative images are shown. The serum levels of (**e**) cTnI, (**f**) TNF-α and (**g**) IL-1β were measured using ELISA. Data are presented as the mean ± SD of data from three independent experiments ($^{*}p < 0.05$, $^{**}p < 0.01$). *NC* normal, *CLP* cecal ligation and puncture, *HSP70* heat shock protein 70, *ECG* echocardiography, *EF* ejection fraction, *Pre-opera.* preoperation, *Post-opera.* postoperation, *cTnI* cardiac troponin I, *TNF-α* tumor necrosis factor-α, *IL-1β* interleukin-1β, *ELISA* enzyme-linked immunosorbent assay, *SD* standard deviation

Immunoprecipitation assays

To detect the endogenous interaction of HSP70 and NLRP3, LPS-treated and LPS + ATP-treated H9C2 cells were lysed and incubated with 3 μg of anti-IgG (ab172730, Abcam) or anti-HSP70 (ab5442, Abcam) antibody and 20 μl of protein A/G beads overnight at 4°C. After centrifugation at 1000 × g for 3 min, the precipitates were collected and analyzed by western blot (WB).

Reverse transcription-quantitative PCR

TRIzol Reagent (Invitrogen, USA) was used to isolate total RNA. A Prime Script™ RT Master Mix kit (Takara, Kusatsu, Shiga, Japan) was used for reverse transcription (RT). PCR was performed using a SYBR Green PCR Kit (Qiagen, Valencia, CA, USA). The sequences of the primers, purchased from Sangon Biotech (Shanghai, China), were as follows: forward primer (F1): 5′ CGCGGATCCATGGACTACAAG-

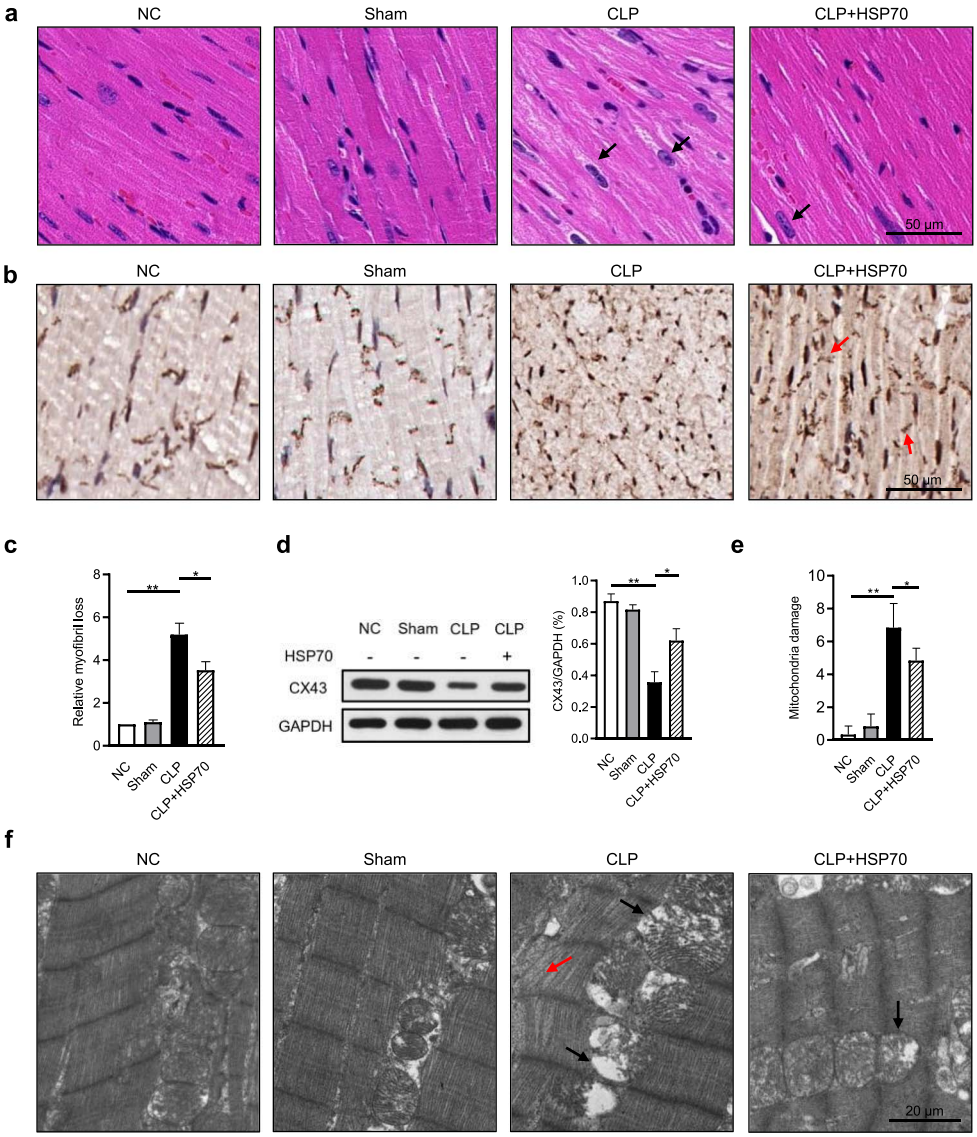

Figure 2. HSP70 attenuates cardiac damage in sepsis-induced cardiomyopathy *in vivo*. Morphological changes in cardiac tissue were observed by (**a**) H&E staining and (**b**) CX43 staining; arrows indicate cytoplasmic vacuolization and cardiomyocyte disorganization. (**c**) The relative myofibril loss was measured by ImageJ. (**d**) The levels of CX43 were determined by western blot. (**e, f**) TEM images, black arrows indicate enlarged mitochondria with vacuolization, red arrow shows disintegrating myofibrils, and the number of damaged mitochondria was measured. Data are presented as the mean ± SD of data from three independent experiments ($^{*}p < 0.05$, $^{**}p < 0.01$). *NC* normal, *CLP* cecal ligation and puncture, *HSP70* heat shock protein 70, *H&E* hematoxylin–eosin, *CX43* connexin 43, *TEM* transmission electron microscopy, *SD* standard deviation

GACGACGATGATAAGGAA −3′; reverse primer (R1): 5′AAGGAAAAAAGCGGCCGCCTAATCTACCTCCTCAA TGGTAGG −3′.

Statistical analysis

Data are presented as the mean ± SD. All data were analyzed using GraphPad Prism version 8.0 software (GraphPad, San Diego, CA, USA). Survival analysis was carried out by the log-rank test. Other results were analyzed by one-way analysis of variance (ANOVA) with Tukey's *post hoc* test. *P* values < 0.05 were considered significant.

Results

HSP70 attenuates cardiac damage in SIC *in vivo*

To determine the protective effect of HSP70 in cardiac injury by sepsis, we created a sepsis mouse model by CLP, and mouse cardiac damage was evaluated grossly and histologically. The gross changes in the CLP animals indicated poor condition with reduced consciousness and activity, liparotrichia, and abundant periocular secretions at 24 h post-CLP, while there were no obvious changes in the normal and sham groups. The changes in CLP mice were alleviated by treatment with exogenous HSP70 (Figure 1a). The survival rates of mice in the sham, CLP and CLP plus HSP70 groups were

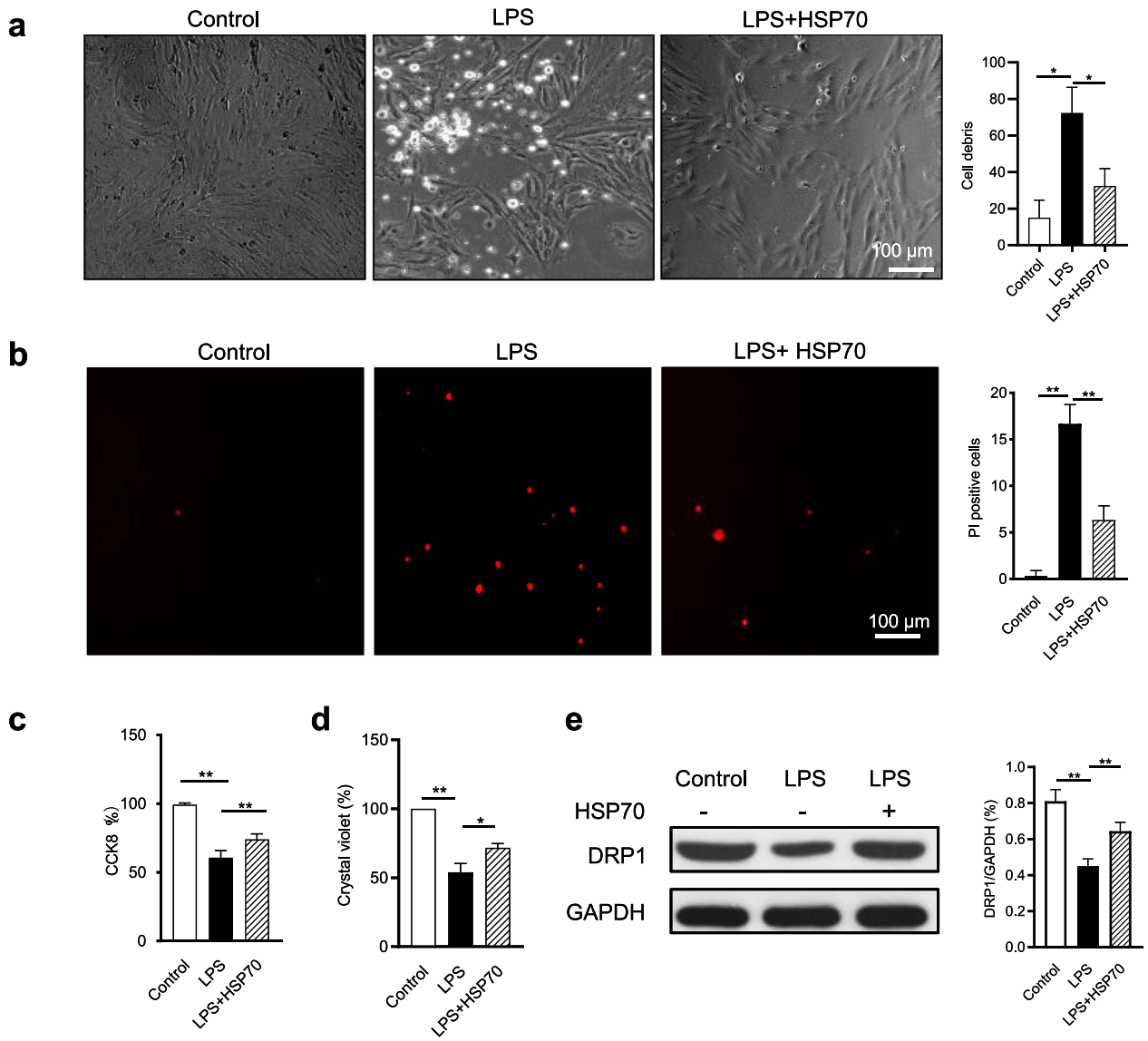

Figure 3. HSP70 improves sepsis-induced cardiomyopathy *in vitro*. H9C2 cells following LPS with/without HSP70 treatment to construct the septic model. (**a**) Cell morphology was observed and the amount of cell debris was calculated. (**b**) Cell viability measured by PI staining. Cell proliferation measured by (**c**) CCK8 and (**d**) crystal violet staining. (**e**) Levels of DRP1 determined by WB. Data are presented as the mean ± SD of data from three independent experiments (*$p < 0.05$, **$p < 0.01$). *LPS* lipopolysaccharide, *HSP70* heat shock protein 70, *PI* propidium iodide, *CCK8* Cell Counting Kit-8, *DRP1* dynamin-related protein 1, *WB* western blot, *SD* standard deviation

clearly lower than those in the normal group. Compared to that in the CLP alone group, the survival rate in the CLP plus HSP70 group was significantly higher, suggesting that HSP70 intervention elevates the survival rate induced by sepsis ($p < 0.05$, Figure 1b). To assess the impact of sepsis on cardiac function, echocardiography (ECG) was performed to measure the ejection fraction (EF) of mice on day 1. The EF, which measures LV blood ejection in the heart, was significantly reduced in the CLP animals ($p < 0.01$) compared to that in the normal and sham groups, demonstrating decreased heart function. Interestingly, this reduced EF was improved in CLP mice treated with HSP70 ($p < 0.05$, Figure 1c, d). To diagnose acute coronary syndromes, we measured the level of cardiac enzymes cTnI and TNF-α (proinflammatory mediator) and IL-1β (pyroptotic marker) in all groups. Our data reveal that CLP animals had significantly higher levels of cTnI, TNF-α and IL-1β than normal and sham animals ($p < 0.01$). These increased levels were decreased with HSP70 treatment ($p < 0.05$, Figure 1e–g). To corroborate our aforementioned data, staining with H&E and gap junctional protein CX43 and transmission electron microscopy (TEM) were performed to observe the cardiac tissue structures. Histologic examination and CX43 staining showed that cardiomyocyte disorganization, cytoplasmic vacuolization, myofibril loss and stromal edema were increased dramatically in the CLP group vs the control group, whereas remarkable reductions in these parameters were observed upon HSP70 treatment (Figure 2a–c). CX43 levels in the

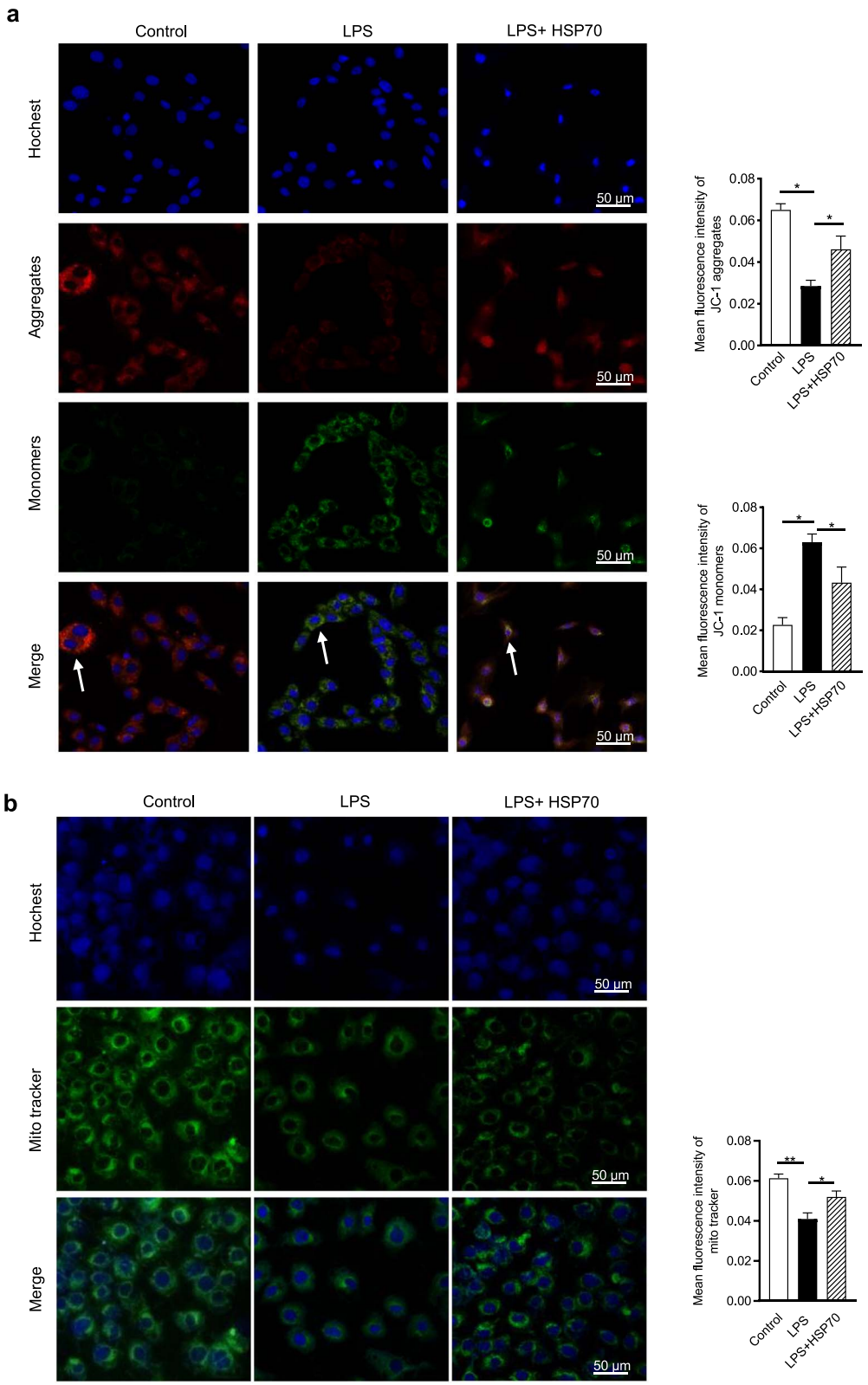

Figure 4. HSP70 ameliorates LPS-induced mitochondrial damage in cardiomyocytes. IF staining was performed to evaluate mitochondrial destabilization, and mitochondrial membrane permeability in cardiomyocytes was assessed by (**a**) JC-1 and (**b**) MitoTracker. JC-1 is a membrane-permeable lipophilic dye that exists as J-aggregates in the mitochondrial matrix (red fluorescence) and as monomers in the cytoplasm (green fluorescence). MitoTracker probes (green fluorescence) can diffuse the dye through the cell membrane and accumulate in active mitochondria. The Hoechst dye stained blue. The fluorescence intensity was calculated by ImageJ. Data are presented as the mean ± SD of data from three independent experiments (* $p < 0.05$, ** $p < 0.01$). *LPS* lipopolysaccharide, *HSP70* heat shock protein 70, *IF* immunofluorescence, *SD* standard deviation

CLP group were upregulated, and these increased levels were decreased with HSP70 treatment ($p < 0.05$, Figure 2d). The TEM results show that samples from the CLP mice had enlarged mitochondria with vacuolization and disintegrating myofibrils; however, these changes were improved by HSP70 treatment (Figure 2e, f). Taken together, our data suggest that cardiac tissue damage develops by CLP-induced sepsis and that HSP70 ameliorates septic cardiomyopathy and elevates the survival rate of CLP mice.

HSP70 improves cell viability and mitochondrial damage induced by LPS in cardiomyocytes

LPS is the main component of the cell wall of most gram-negative bacteria and is often used to induce inflammation. To elucidate the mechanisms of sepsis-induced myocardial dysfunction, H9C2 cells were used to establish a model of sepsis-induced myocardial dysfunction using LPS stimulation *in vitro*. The H9C2 cell morphology showed that LPS caused H9C2 cells to shrink and separate (Figure 3a). The cell viability results indicate that LPS promoted cell death, as shown by PI staining, CCK8 and crystal violet staining, respectively. HSP70 treatment improved H9C2 cell morphology and ameliorated the reduced cell viability induced by LPS (Figure 3b–f). Emerging evidence suggests that one of the main causes of SIC is mitochondrial dysfunction of cardiomyocytes, which leads to the initiation of cell death by pyroptosis through activation of the NLRP3 inflammasome. Next, we assessed mitochondrial destabilization in H9C2 cells. DRP1 expression was measured by WB to detect mitochondrial function (Figure 3g). The level of DRP1 increased after LPS treatment. Hsp70 effectively downregulated DRP1 expression in the LPS group ($p < 0.05$). Immunofluorescence (IF) staining with JC-1 and MitoTracker was performed to evaluate the mitochondrial membrane potential in cardiomyocytes following LPS with/without HSP70 treatment. The presence of JC-1 aggregates and MitoTracker in H9C2 cells was significantly ($p < 0.01$) decreased in the LPS-treated group compared with the control. However, treatment with HSP70 significantly reduced the number of JC-1 aggregate-positive cells (Figure 4a–c) and MitoTracker-positive cells (Figure 4d, e). In comparison, an increasing trend of JC-1 monomers was observed after LPS stimulation, and this trend was reversed upon treatment with HSP70. Altogether, these results suggest that H9C2 cells treated with LPS exhibit mitochondrial destabilization and damage by inducing loss of mitochondrial membrane potential and increased permeability of the membrane, and that HSP70 ameliorates mitochondrial damage in H9C2 cells and suppresses cell death.

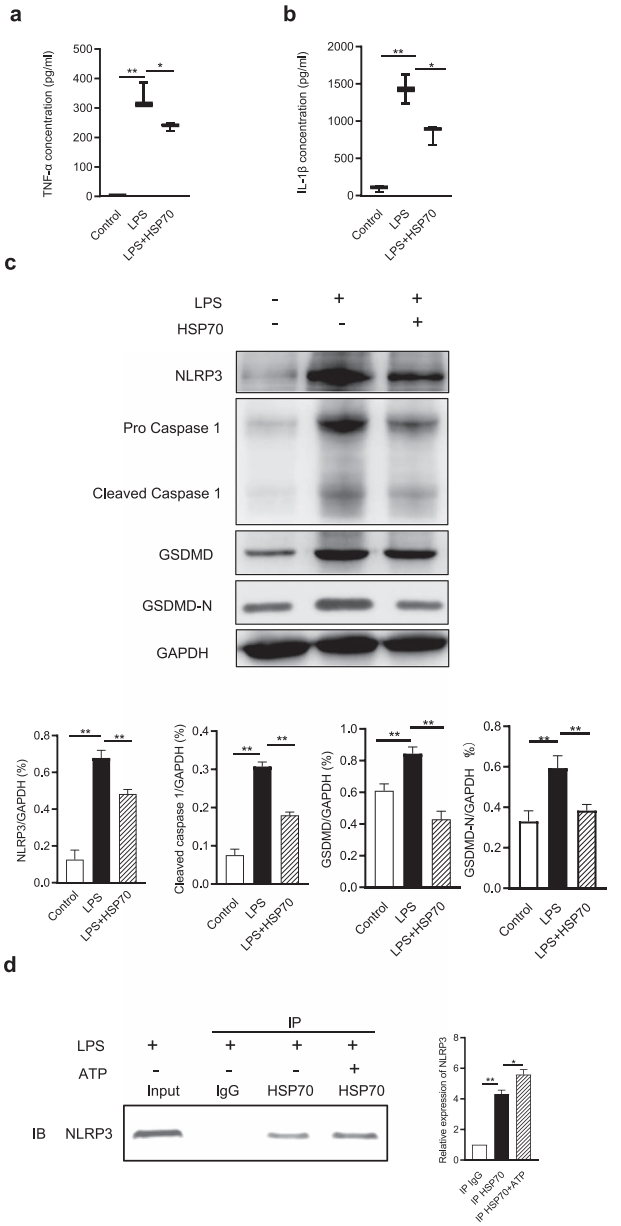

Figure 5. HSP70 effects on inflammation and pyroptosis *in vitro*. Protein levels of the inflammatory cytokines (**a**) TNF-α and (**b**) IL-1β determined using ELISA. (**c**) The levels of pyroptosis-related proteins (NLRP3, caspase-1, GSDMD, GSDMD-N) determined by WB. (**d**) LPS-primed H9C2 cells treated or not with ATP were lysed and immunoprecipitated with HSP70 antibody, and NLRP3 protein was measured by WB using NLRP3 antibody. Data are presented as the mean ± SD of data from three independent experiments ($^{*}p < 0.05$, $^{**}p < 0.01$). *LPS* lipopolysaccharide; *HSP70* heat shock protein 70, *TNF-α* tumor necrosis factor-α, *IL-1β* interleukin-1β, *ELISA* enzyme-linked immunosorbent assay, *NLRP3* nucleotide-binding domain, leucine-rich-repeat containing family pyrin domain-containing 3, *GSDMD* gasdermin-D, *GSDMD-N* gasdermin-D N-terminal, *IP* immunoprecipitation, *IB* immunoblotting, *WB* western blot, *SD* standard deviation

HSP70 inhibits LPS-induced pyroptosis by repressing the NLRP3/caspase-1/GSDMD signaling pathway in cardiomyocytes

Published studies suggest that inflammatory responses lead to the induction of proinflammatory cytokines, such as TNF-α and IL-1β, or the activation of caspase-1, resulting in NLRP3 inflammasome-mediated pyroptosis. To understand whether NLRP3 inflammasome protein formation can initiate pyroptosis in SIC, we determined the levels of

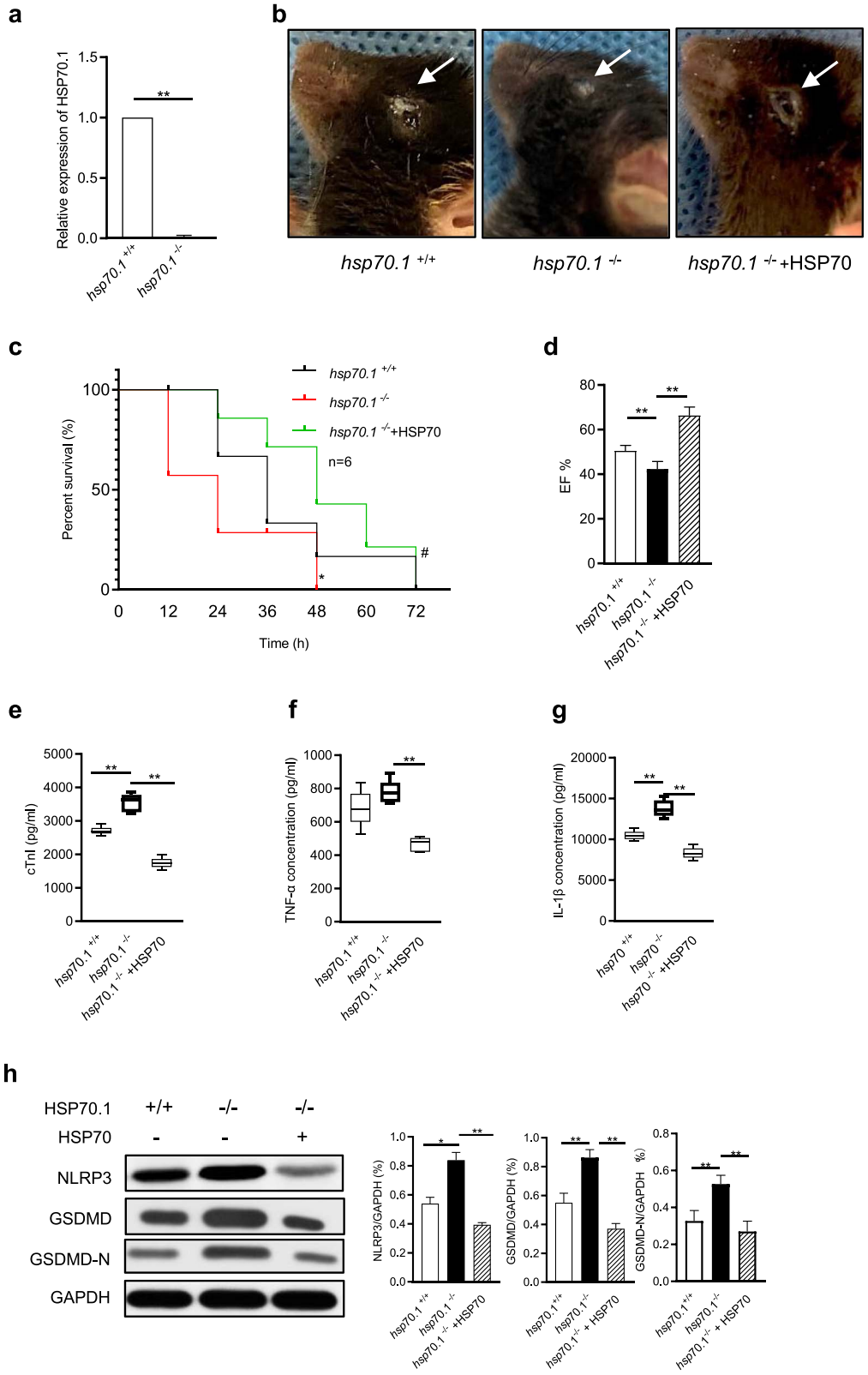

Figure 6. HSP70 gene deficiency in sepsis-induced inflammation and NLRP3 inflammasome–caspase-1–GSDMD and pyroptosis *in vivo*. (**a, b**) The relative RNA expression level of HSP70.1 in $hsp70.1^{+/+}$ and $hsp70.1^{-/-}$ mice measured by RT-PCR $hsp70.1^{+/+}$ and $hsp70.1^{-/-}$ mice were treated with CLP with/without HSP70 to assess the gross profile and periocular secretions as indicated with white arrows. (**c**) Survival rates were observed ($^{*}p < 0.05$, $hsp70.1^{+/+}$ *vs* $hsp70.1^{-/-}$, $\#p < 0.05$, $hsp70.1^{-/-}$ *vs* $hsp70.1^{-/-}$ + HSP70). (**d**) ECG was performed to measure the ejection fraction. Levels of the cardiac enzyme (**e**) cTnI and the inflammatory factors (**f**) TNF-α and (**g**) IL-1β measured using ELISA. (**h**) The level of pyroptosis-related protein was confirmed by WB. Data are presented as the mean ± SD of data from three independent experiments ($^{*}p < 0.05$, $^{**}p < 0.01$). *RT-PCR* reverse transcription-quantitative polymerase chain reaction, *CLP* cecal ligation and puncture, *HSP70* heat shock protein 70, *ECG* echocardiography, *EF* ejection fraction, *cTnI* cardiac troponin I, *TNF-α* tumor necrosis factor-α, *IL-1β* interleukin-1β, *ELISA* enzyme-linked immunosorbent assay, *WB* western blot, *SD* standard deviation

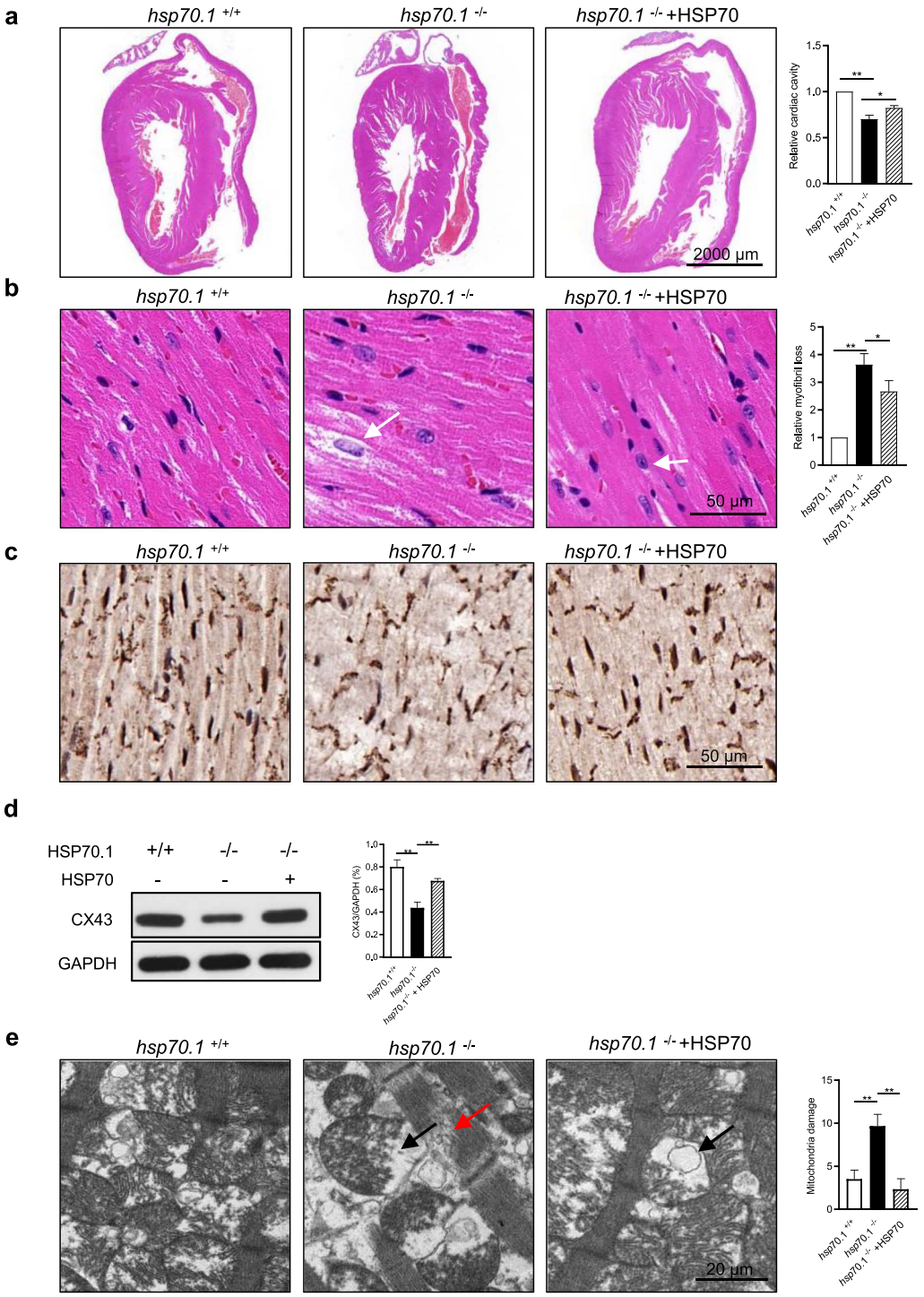

Figure 7. HSP70 deficiency aggravates sepsis-induced cardiomyopathy *in vivo*. *hsp70.1*$^{+/+}$ and *hsp70.1*$^{-/-}$ mice were treated with CLP with/without HSP70. (**a**) The relative cardiac cavity was calculated by ImageJ from the H&E staining gross view. (**b**) White arrows show cytoplasmic vacuolization and relative myofibril loss was measured by ImageJ. (**c**) CX43 staining of cardiac tissue. (**d**) Levels of CX43 determined by WB. (**e**) TEM showed enlarged mitochondria with vacuolization (black arrow) and disintegrating myofibrils (red arrow) and the number of damaged mitochondria was measured. Data are presented as the mean ± SD of data from three independent experiments (*$p < 0.05$, **$p < 0.01$). *CLP* cecal ligation and puncture, *H&E staining* hematoxylin–eosin staining, *CX43* connexin 43, *TEM* transmission electron microscopy, *SD* standard deviation

TNF-α-, IL-1β- and classical caspase-1-dependent pyroptosis pathways in H9C2 cells. First, our data show that the protein levels of TNF-α and IL-1β were enhanced by LPS compared with the control group, and these increased cytokines were reduced after HSP70 treatment (Figure 5 a, b, $p < 0.01$). Next, we found that LPS significantly increased the levels of TNF-α and IL-1β and also significantly elevated the protein levels of NLRP3, caspase-1, cleaved caspase-1, GSDMD

and GSDMD-N compared with the control (Figure 5c, $p < 0.01$, $p < 0.05$). Furthermore, exogenous HSP70 repressed the levels of NLRP3 inflammasome-mediated proteins that were increased by LPS. To further verify the interaction between HSP70 and NLRP3 in H9C2 cells, we performed immunoprecipitation and immunoblotting analyses with antibodies against HSP70 and NLRP3. An obvious band of HSP70–NLRP3 was observed in H9C2 cells treated with LPS plus ATP (Figure 5d). Collectively, these results demonstrate that HSP70 inhibits proinflammatory cytokines and inactivates pyroptotic signaling pathway molecules, including NLRP3, cleaved caspase-1, GSDMD and GSDMD-N, leading to reduced pyroptosis in cardiomyocytes *in vitro*.

HSP70 deficiency aggravates cardiac damage in sepsis-induced cardiomyopathy by regulating pyroptosis through activation of the NLRP3 inflammasome/caspase-1/GSDMD pathway

To strengthen and confirm our data on inflammasome activation-mediated pyroptosis *in vivo*, *hsp70.1*$^{-/-}$ mice were utilized to create a septic model by CLP. The levels of HSP70.1 dramatically decreased in *hsp70.1*$^{-/-}$ mice, as shown by RT-PCR (Figure 6a). Gross observations showed that *hsp70.1*$^{-/-}$ mice were prone to suffering from CLP injury compared to *hsp70.1*$^{+/+}$ mice, including reduced activity, liparotrichia, abundant periocular secretions, worse response to stimulus and mostly closed eyes (Figure 6b). In addition, a lower survival rate was observed in *hsp70.1*$^{-/-}$ mice (Figure 6c). These changes in *hsp70.1*$^{-/-}$ CLP mice were ameliorated by treatment with exogenous HSP70. Moreover, the cardiac functions and cytokines of mice were evaluated by ECG and ELISA. The EF of the heart in *hsp70.1*$^{-/-}$ CLP mice was significantly suppressed compared with that in *hsp70.1*$^{+/+}$ CLP animals (Figure 6d, $p < 0.05$). The levels of cTnI, IL-1β and TNF-α in the serum of HSP gene knockout mice were markedly higher than those in the WT mice (Figure 6e–g, $p < 0.01$), suggesting that gene deletion of HSP70 results in cardiac dysfunction and increased inflammation. Meanwhile, inflammasome activation-mediated proteins were determined and the results reveal that the levels of NLRP3, GSDMD and GSDMD-N were enhanced in gene deletion mice compared with those in WT animals (Figure 6h). H&E and CX43 staining were used to examine the histological changes in myocardial tissues and it was found that the cardiac cavity in *hsp70.1*$^{-/-}$ CLP mice was much smaller than that in *hsp70.1*$^{+/+}$ CLP mice, myocardial fiber bundles were lost and dissolved, some cardiomyocytes were vacuolized and stromal edema was noted in *hsp70.1*$^{-/-}$ mice after CLP (Figure 7a–c, $p < 0.05$). CX43 expression showed a similar result (Figure 7d). TEM observations revealed enlarged mitochondria with vacuolization and disintegrating myofibrils in myocardial tissues in *hsp70.1*$^{-/-}$ CLP animals compared to WT CLP mice (Figure 7e). In contrast, *hsp70.1*$^{-/-}$ CLP mice treated with exogenous HSP70 showed significant reversal of these changes. Overall, these data support that HSP70 plays a critical role in SIC by inactivating the pyroptosis-related NLRP3 inflammasome signaling pathway.

Discussion

In the present study, we established a sepsis-induced cardiomyopathy model using CLP mice and LPS-stimulated H9C2 cells to observe heart function, myocardial structure, mitochondrial stabilization, inflammation and pyroptosis *in vivo* and *in vitro*. The results show a lower survival rate in septic mice with poor general condition. The ECG results indicate that EF by ECG was reduced and cTnI in the serum elevated as time progressed in the 24 h post-CLP. Under a microscope, myocardial tissue in the sepsis model exhibited myocardial fiber rupture and edema, enlarged mitochondria with vacuolization and disintegrating myofibrils. In addition, the protein levels of TNF-α and IL-1β, activation of the NLRP3 inflammasome, cleavage of caspase-1, cleavage of GSDMD and cell death were increased in the animal and cell models of sepsis. Interestingly, treatment with HSP70 remarkably repaired sepsis-induced myocardial damage by improving mitochondrial destabilization and attenuating the activation of NLRP3 inflammasome-mediated pyroptosis. Conversely, deletion of the HSP70 gene inhibited these events and led to increased mortality after sepsis initiation due to its upregulation in NLRP3 inflammasome-mediated pyroptosis. These findings define a potentially vital mechanism by which the heat stress protein HSP70 can protect against septic damage in myocardial tissue.

The role of mitochondria has been gaining increasing attention as a key contributor to the pathophysiology of SIC [31,32]. In this study, we successfully established an SIC model in mice, as evidenced by the changes in cTnI (a specific marker for the diagnosis of myocardial injury), EF of cardiac function and myocardial tissue histology. In addition, we measured the mitochondrial morphology and membrane potential by TEM and IF, respectively. Sepsis decreased cardiac mitochondrial membrane potential and stabilization and resulted in structural abnormalities *in vivo* and *in vitro*, suggesting that mitochondrial dysfunction occurred in cardiomyocytes. Our results are consistent with other reports that demonstrated sepsis-induced abnormalities of mitochondrial structure, such as swelling and loss or disruption of cristae and disruption of the inner and outer membranes in cardiac mitochondria in animals and patients. Hence, mitochondrial dysfunction has internal connections with the pathogenesis of SIC [30,33,34]. Excessive mitochondrial destabilization has been shown to induce changes in mitochondrial membrane potential in a variety of disease models, such as ischemia/reperfusion and neurodegenerative diseases [35]. We also showed that HSP70 treatment improved pathological mitochondrial dysfunction and rescued cardiac function in a cardiac cell line model with sepsis. However, little is known about the mechanism of this event. Therefore, it is necessary to determine whether mitochondrial dysfunction is associated with activation

of the NLRP3 inflammasome-mediated signaling pathway and promotion of pyroptosis of cardiomyocytes after LPS stimulation. Within the limits of this study, more evidence is needed to prove that extracellular HSP70 was taken up by cardiomyocytes.

Emerging evidence reveals that mitochondria play a pivotal role in the initiation and activation of the NLRP3 inflammasome by releasing mitochondria-derived molecules such as cardiolipin and mitochondrial DNA after destabilization [12]. Importantly, these molecules can bind to NLRP3 and activate the NLRP3 inflammasome [36,37]. The NLRP3 inflammasome has recently gained close attention in SIC. It comprises three main members, including apoptosis-associated speck-like protein, NLRPs and an adaptor that enables the recruitment and activation of proinflammatory caspases such as caspase-1. NLRP3 is a vital mediator in inflammasome formation and initiation of the immune response, which can be induced by mitochondrial-mediated DAMPs or PAMPs. The NLRP3 inflammasome induces the secretion of proinflammatory cytokines, such as TNF-α and IL-1β, and the activation of caspase-1, resulting in GSDMD-mediated pyroptosis or inflammation. In our study, the levels of NLRP3 in both cardiac tissue and H9C2 cells were increased dramatically after septic stimulation. Moreover, we found that the levels of TNF-α and IL-1β in serum and the activation of caspase-1 and GSDMD were also elevated in CLP mice and LPS-treated cardiomyocytes. A previous study revealed that increased TNF-α and IL-1β by NLRP3 inflammasome activation could further amplify inflammation in various models, such as in a pulmonary infection and the brains of mice after alcohol administration [21,38]. In addition, we found that caspase-1 activation and GSDMD increased in mice and H9C2 cells after sepsis. Caspase-1 cleavage induced by the NLRP3 inflammasome is involved in rapid lytic cell death termed pyroptosis, which may not be responsible for apoptosis. GSDMD is one of the most important mediators of pyroptosis and mice with GSDMD depletion are resistant to LPS-induced lethal death [39]. The NLRP3 inflammasome regulates the inflammatory response and pyroptosis has been shown to play essential roles in some diseases, such as acute kidney injury induced by sepsis [40]. Caspase-1 is activated within the canonical inflammasome and mediates proinflammatory factors, such as TNF-a, IL-1β and IL-6, leading to local and systemic inflammation [41]. Consistent with their study, we found that LPS triggered the activation of NLRP3 and caspase-1 and increased GSDMD and pyroptosis in H9C2 cells. Moreover, the NLRP3–caspase-1–GSDMD inflammasome axis contributes to sepsis-induced cardiac dysfunction in both mice and cells.

After determining the mitochondria-initiated activation of the NLRP3 inflammasome–pyroptosis pathway in SIC, we further determined whether HSP70 has a protective effect on cardiac dysfunction following septic stimulation. Interestingly, our data show that HSP70 administration attenuated mitochondrial destabilization and inhibited NLRP3 inflammasome-mediated inflammation and cell death, indicating that HSP70 is essential in the regulation of NLRP3 inflammasome activation. SIC is caused by a systemic inflammatory response due to infection, followed by dysfunction of the heart. Inflammatory mediators (e.g. TNF-α and IL-1β) play important roles in the development of SIC, as they can lead to cascade reactions and further amplification of inflammatory signals [42]. HSP70 has been noted to inhibit inflammation via several mechanisms, including limiting NF-κB activation and impairing apoptotic cellular pathways [43,44]. Additionally, some studies have shown that HSP70 downregulates cardiomyocyte necroptosis by suppressing autophagy and protects cardiomyocytes by inhibiting SUMOylation and nuclear translocation of phosphorylated eukaryotic elongation factor 2 in myocardial ischemia [45]. Our results suggest an unexpected mechanism in which HSP70 protects against CLP in mice and cell death in H9C2 cells by suppressing mitochondrial dysfunction and NLRP3 inflammasome activation. HSP70 gene deletion increased mitochondrial dysfunction and NLRP3 inflammasome activation, leading to activation of caspase-1 and IL-1β and increasing pyroptosis. The inhibitory role of HSP70 may, at least partly, be due to its interaction with NLRP3.

To our knowledge, this is the first time that HSP70 knockout has been shown to promote animal death and mitochondrial dysfunction and inactivate the NLRP3 inflammasome/caspase-1/GSDMD signaling pathway, and that exogenous HSP70 rescued septic cardiac tissue damage by suppressing mitochondrial dysfunction, NLRP3 inflammasome activation and pyroptosis during sepsis-induced cardiomyopathy.

Conclusions

The results of this study demonstrate that mitochondrial destabilization and NLRP3 activation-mediated pyroptosis in cardiac tissue are attributed to sepsis-induced cardiomyopathy. Additionally, HSP70 ameliorates sepsis-induced myocardial dysfunction by improving mitochondrial dysfunction and inhibiting inflammasome-mediated pyroptosis activation. Our findings indicate that exogenous HSP70 might be a potential therapeutic strategy for sepsis-induced cardiomyopathy.

Abbreviations

CCK8: Cell Counting Kit-8; CLP, Cecal ligation plus perforation; cTnI: Cardiac troponin I; DAMPs: Danger-associated molecular patterns; DRP1: Dynamin-related protein 1; ELISA: Enzyme-linked immunosorbent assay; GSDMD: Gasdermin-D; H&E: Hematoxylin and eosin; HSP: Heat shock protein; IF: immunofluorescence; IL-1β: Interleukin-1β; LPS: Lipopolysaccharide; NLRP3: Nucleotide-binding domain, leucine-rich-repeat containing family pyrin domain-containing 3 ; RT-PCR, Reverse transcription polymerase chain reaction; SIC: Sepsis-induced cardiomyopathy; TEM, Transmission electron microscopy; TNF-α: Tumor necrosis factor-α: WB, Western blot.

Acknowledgments

We would like to acknowledge Dr. Yong Hu and Dr. Lei Zheng for kindly providing experimental support and Dr. Haibin Zhang for constructive suggestions.

Funding

This study was supported by the National Natural Science Foundation of China (81772118).

Authors' contributions

CLS and YQZ performed the study, analyzed the data and drafted the manuscript. QP, WN and WZ performed the animal experiments. LZ, MYW and YZS performed the echocardiography. SW analyzed the data. XJF and YBP edited the manuscript. MY designed the study, revised the manuscript and provided funding support. All authors have given final approval and agree to be accountable for all aspects of the work.

Ethics approval and consent to participate

The animal study was approved by the Animal Research Committee of the Shanghai Jiao Tong University School of Medicine (Number: HKDL-2017-316).

Data availability

The datasets used and/or analyzed in the current study are available from the corresponding author upon reasonable request.

Conflicts of interest

The authors state no conflict of interest.

References

1. Singer M, Deutschman CS, Seymour CW, Shankar-Hari M, Annane D, Bauer M, *et al*. The third international consensus definitions for sepsis and septic shock (Sepsis-3). *JAMA*. 2016; 315:801–10.
2. Zaky A, Deem S, Bendjelid K, Treggiari MM. Characterization of cardiac dysfunction in sepsis: an ongoing challenge. *Shock*. 2014;41:12–24. https://doi.org/10.1097/SHK.0000000000000065:\protect$\relax^\wedge$10.1097/SHK.0000000000000065.
3. Kakihana Y, Ito T, Nakahara M, Yamaguchi K, Yasuda T. Sepsis-induced myocardial dysfunction: pathophysiology and management. *J Intensive Care*. 2016;4:22. https://doi.org/10.1186/s40560-016-0148-1.
4. Zaky A, Deem K, Fau-Bendjelid S, Bendjelid MM, Fau-Treggiari K, Treggiari MM. Characterization of cardiac dysfunction in sepsis: an ongoing challenge. *Shock*. 2014;41:12–24.
5. Rocha M, Herance S, Fau-Rovira R, Rovira A, Fau-Hernández-Mijares S, Hernández-Mijares VM, *et al*. Mitochondrial dysfunction and antioxidant therapy in sepsis. *Infect Disord Drug Targets*. 2012;12:161–78.
6. Kang R, Zeng L, Zhu S, Xie Y, Liu J, Wen Q, *et al*. Lipid peroxidation drives Gasdermin D-mediated Pyroptosis in lethal Polymicrobial sepsis. *Cell Host Microbe*. 2018;24:97–108.
7. Yu X, Jia F, Fau-Wang B, Wang X, Fau-Lv F, Lv X, *et al*. α_1 adrenoceptor activation by norepinephrine inhibits LPS-induced cardiomyocyte TNF-α production via modulating ERK1/2 and NF-κB pathway. *J Cell Mol Med*. 2014;18:263–73.
8. Wang Y, Wang Y, Yang D, Yu X, Li H, Lv X, *et al*. β_1-adrenoceptor stimulation promotes LPS-induced cardiomyocyte apoptosis through activating PKA and enhancing CaMKII and IκBα phosphorylation. *Crit Care*. 2015;19:76. https://doi.org/10.1186/s13054-015-0820-1.
9. Yi RF, Lin JZ, Cui L, Zhang Q, Jia JZ, Lyu YL, *et al*. Role of hexokinase II in the changes of autophagic flow in cardiomyocytes of mice with ischemia-hypoxia in vitro. *Zhonghua Shao Shang Za Zhi*. 2019;35:116–24.
10. Shi J, Gao W, Shao F. Pyroptosis: Gasdermin-mediated programmed necrotic cell death. 2017;42:245–54.
11. Xiang F, Xue DD, Luo J, Hu JH, Yuan LL, Jia JZ, *et al*. Effects and mechanism of mitochondrial transcription factor a and cytochrome c oxidase pathway in the energy production of hypoxic cardiomyocytes of rats regulated by tumor necrosis factor receptor associated protein 1. *Zhonghua Shao Shang Za Zhi*. 2020;36:651–7.
12. Zhou R, Yazdi AS, Menu P, Tschopp J. A role for mitochondria in NLRP3 inflammasome activation. *Nature*. 2011;469:221–5. https://doi.org/10.1038/nature09663:^10.1038/nature09663.
13. Kelley N, Jeltema D, Duan Y, He Y. The NLRP3 Inflammasome: an overview of mechanisms of activation and regulation. *Int J Mol Sci*. 2019;20:3328. https://doi.org/10.3390/ijms20133328.
14. Sun L, Ma W, Gao W, Xing Y, Chen L, Xia Z, *et al*. Propofol directly induces caspase-1-dependent macrophage pyroptosis through the NLRP3-ASC inflammasome. *Cell Death Dis*. 2019;10:542. https://doi.org/10.1038/s41419-019-1761-4.
15. Qiu Z, Lei S, Zhao B, Wu Y, Su W, Liu M, *et al*. NLRP3 Inflammasome activation-mediated Pyroptosis aggravates myocardial ischemia/reperfusion injury in diabetic rats. *Oxidative Med Cell Longev*. 2017;2017:9743280. https://doi.org/10.1155/2017/9743280.
16. Fernández-Fernández MR, Valpuesta JM. Hsp70 chaperone: a master player in protein homeostasis. *F1000Res*. 2018;7:F1000. Faculty Rev-1497. https://doi.org/10.12688/f1000research.15528.1.
17. Nillegoda NB, Kirstein J, Szlachcic A, Berynskyy M, Stank A, Stengel F, *et al*. Crucial HSP70 co-chaperone complex unlocks metazoan protein disaggregation. *Nature*. 2015;524:247–51. https://doi.org/10.1038/nature14884:^10.1038/nature14884.
18. Leu JI, Barnoud T, Zhang G, Tian T, Wei Z, Herlyn M, *et al*. Inhibition of stress-inducible HSP70 impairs mitochondrial proteostasis and function. *Oncotarget*. 2017;8, 28:45656–69. https://doi.org/10.18632/oncotarget.17321.
19. Yuan, Z.Q., X.L. Li, Y.Z. Peng, P. Wang, Y.S. Huang, and Z.C. Yang, [Influence of HSP70 on function and energy metabolism of mitochondria in intestinal epithelial cells after hypoxia/reoxygenation]. *Zhonghua Shao Shang Za Zhi*, 2008. 24(3): p. 203–6.
20. Stankiewicz, A.R., G. Lachapelle, C.P. Foo, S.M. Radicioni, and D.D. Mosser, Hsp70 inhibits heat-induced apoptosis upstream of mitochondria by preventing Bax translocation. *J Biol Chem*, 2005. 280(46): p. 38729–39.
21. Rumora L, Hlapčić I, Hulina-Tomašković A, Somborac-Bačura A, Bosnar M, Rajković MG. Pathogen-associated molecular patterns and extracellular Hsp70 interplay in NLRP3 inflammasome activation in monocytic and bronchial epithelial cellular models of COPD exacerbations. *APMIS*. 2021;129: 80–90.

22. Hawiger J, Veach RA, Zienkiewicz J. New paradigms in sepsis: from prevention to protection of failing microcirculation. *J Thromb Haemost*. 2015;13:1743–56.
23. Wang X, Zhu Y, Zhou Q, Yan Y, Qu J, Ye H. Heat shock protein 70 expression protects against sepsis-associated cardiomyopathy by inhibiting autophagy. *Hum Exp Toxicol*. 2021;40:735–41.
24. Vicencio JM, Yellon DM, Sivaraman V, Das D, Boi-Doku C, Arjun S, *et al*. Plasma exosomes protect the myocardium from ischemia-reperfusion injury. *J Am Coll Cardiol*. 2015; 65:1525–36.
25. Wick G, Knoflach M, Xu Q. Autoimmune and inflammatory mechanisms in atherosclerosis. *Annu Rev Immunol*. 2004;22: 361–403. https://doi.org/10.1146/annurev.immunol.22.012703.104644:^10.1146/annurev.immunol.22.012703.104644.
26. Dybdahl B, Slørdahl SA, Waage A, Kierulf P, Espevik T, Sundan A. Myocardial ischaemia and the inflammatory response: release of heat shock protein 70 after myocardial infarction. *Heart*. 2005;91:299–304.
27. Gromadzka G, Zielińska J, Ryglewicz D, Fiszer U, Członkowska A. Elevated levels of anti-heat shock protein antibodies in patients with cerebral ischemia. *Cerebrovasc Dis*. 2001;12: 235–9.
28. Konstantinova EV, Chipigina NS, Shurdumova MH, Kovalenko EI, Sapozhnikov AM. Heat shock protein 70 kDa as a target for diagnostics and therapy of cardiovascular and cerebrovascular diseases. *Curr Pharm Des*. 2019;25:710–4.
29. Wei S, Gao Y, Dai X, Fu W, Cai S, Fang H, *et al*. SIRT1-mediated HMGB1 deacetylation suppresses sepsis-associated acute kidney injury. *Am J Physiol Renal Physiol*. 2019;316: F20–f31.
30. Haileselassie B, Mukherjee R, Joshi AU, Napier BA, Massis LM, Ostberg NP, *et al*. Drp1/Fis1 interaction mediates mitochondrial dysfunction in septic cardiomyopathy. *J Mol Cell Cardiol*. 2019;130:160–9.
31. Piquereau J, Godin R, Deschênes S, Bessi VL, Mofarrahi M, Hussain SN, *et al*. Protective role of PARK2/parkin in sepsis-induced cardiac contractile and mitochondrial dysfunction. *Autophagy*. 2013;9:1837–51.
32. Fang X, Wang J. Role of mitochondrial dysfunction in the pathogenesis of septic cardiomyopathy. *Zhonghua Wei Zhong Bing Ji Jiu Yi Xue*. 2018;30:189–92.
33. Bock FJ, Tait SWG. Mitochondria as multifaceted regulators of cell death. *Nat Rev Mol Cell Biol*. 2020;21:85–100.
34. Lin Y, Xu Y, Zhang Z. Sepsis-induced myocardial dysfunction (SIMD): the pathophysiological mechanisms and therapeutic strategies targeting mitochondria. *Inflammation*. 2020;43:1184–200.
35. Paillard M, Tubbs E, Thiebaut PA, Gomez L, Fauconnier J, Da Silva CC, *et al*. Depressing mitochondria-reticulum interactions protects cardiomyocytes from lethal hypoxia-reoxygenation injury. *Circulation*. 2013;128:1555–65.
36. Martine P, Chevriaux A, Derangère V, Apetoh L, Garrido C, Ghiringhelli F, *et al*. HSP70 is a negative regulator of NLRP3 inflammasome activation. *Cell Death Dis*. 2019; 10:256. https://doi.org/10.1038/s41419-019-1491-7:^10.1038/s41419-019-1491-7.
37. Ullah M, Liu DD, Rai S, Concepcion W, Thakor AS. HSP70-mediated NLRP3 Inflammasome suppression underlies reversal of acute kidney injury following extracellular vesicle and focused ultrasound combination therapy. *Int J Mol Sci*. 2020;21:4085. https://doi.org/10.3390/ijms21114085.
38. Qu J, Tao XY, Teng P, Zhang Y, Guo CL, Hu L, *et al*. Blocking ATP-sensitive potassium channel alleviates morphine tolerance by inhibiting HSP70-TLR4-NLRP3-mediated neuroinflammation. *J Neuroinflammation*. 2017;14:228. https://doi.org/10.1186/s12974-017-0997-0.
39. Wang K, Sun Q, Zhong X, Zeng M, Zeng H, Shi X, *et al*. Structural mechanism for GSDMD targeting by autoprocessed caspases in Pyroptosis. *Cell*. 2020;180:941–955.e20.
40. Komada T, Muruve DA. The role of inflammasomes in kidney disease. *Nat Rev Nephrol*. 2019;15:501–20.
41. Neudorf H, Durrer C, Myette-Cote E, Makins C, O'Malley T, Little JP. Oral ketone supplementation acutely increases markers of NLRP3 Inflammasome activation in human monocytes. *Mol Nutr Food Res*. 2019;63:e1801171. https://doi.org/10.1002/mnfr.201801171.
42. Hollenberg SM, Singer M. Pathophysiology of sepsis-induced cardiomyopathy. *Nat Rev Cardiol*. 2021;18:424–34.
43. Vinokurov M, Ostrov V, Yurinskaya M, Garbuz D, Murashev A, Antonova O, *et al*. Recombinant human Hsp70 protects against lipoteichoic acid-induced inflammation manifestations at the cellular and organismal levels. *Cell Stress Chaperones*. 2012;17:89–101.
44. Dokladny K, Lobb W, Fau-Wharton R, Wharton TY, Fau-Ma W, Ma PL, *et al*. LPS-induced cytokine levels are repressed by elevated expression of HSP70 in rats: possible role of NF-kappaB. *Cell Stress Chaperones*. 2010;15: 153–63.
45. Zhang C, Liu X, Miao J, Wang S, Wu L, Yan D, *et al*. Heat shock protein 70 protects cardiomyocytes through suppressing SUMOylation and nucleus translocation of phosphorylated eukaryotic elongation factor 2 during myocardial ischemia and reperfusion. *Apoptosis*. 2017;22: 608–25.